

Video Coding for Machines with Feature-Based Rate-Distortion Optimization

Kristian Fischer, Fabian Brand, Christian Herglotz, André Kaup
Multimedia Communications and Signal Processing

Friedrich-Alexander-Universität Erlangen-Nürnberg (FAU)

Cauerstr. 7, 91058 Erlangen, Germany

{Kristian.Fischer, Fabian.Brand, Christian.Herglotz, Andre.Kaup}@fau.de

Abstract—Common state-of-the-art video codecs are optimized to deliver a low bitrate by providing a certain quality for the final human observer, which is achieved by rate-distortion optimization (RDO). But, with the steady improvement of neural networks solving computer vision tasks, more and more multimedia data is not observed by humans anymore, but directly analyzed by neural networks. In this paper, we propose a standard-compliant feature-based RDO (FRDO) that is designed to increase the coding performance, when the decoded frame is analyzed by a neural network in a video coding for machine scenario. To that extent, we replace the pixel-based distortion metrics in conventional RDO of VTM-8.0 with distortion metrics calculated in the feature space created by the first layers of a neural network. Throughout several tests with the segmentation network Mask R-CNN and single images from the Cityscapes dataset, we compare the proposed FRDO and its hybrid version HFRDO with different distortion measures in the feature space against the conventional RDO. With HFRDO, up to 5.49 % bitrate can be saved compared to the VTM-8.0 implementation in terms of Bjøntegaard Delta Rate and using the weighted average precision as quality metric. Additionally, allowing the encoder to vary the quantization parameter results in coding gains for the proposed HFRDO of up 9.95 % compared to conventional VTM.

Index Terms—Video Coding for Machines, Rate-Distortion Optimization, R-CNN, Versatile Video Coding

I. INTRODUCTION

Nowadays, the amount of multimedia data that is captured to be utilized by machines instead of humans increases significantly. This machine-to-machine (M2M) communication is used for algorithms that independently solve tasks in several scopes of application, e.g., in industrial processes, detecting objects or incidents in surveillance scenarios, or in the emerging field of autonomous driving. With this increasing amount of M2M data, a suitable compression method has to be found in order to reduce the network traffic or required storage space.

Traditional hybrid video codecs like High-efficiency Video Coding (HEVC) [1] and its planned successor Versatile Video Coding (VVC) [2] [3] are highly optimized to deliver the best possible quality at a specific bitrate, for which the final human user is taken as reference to evaluate the quality. Hence, the question arises, whether the optimizations made for the human user also result in the best possible compression when the compressed multimedia data is observed by an algorithm

The authors gratefully acknowledge that this work has been supported by the Deutsche Forschungsgemeinschaft (DFG) under contract number KA 926/10-1.

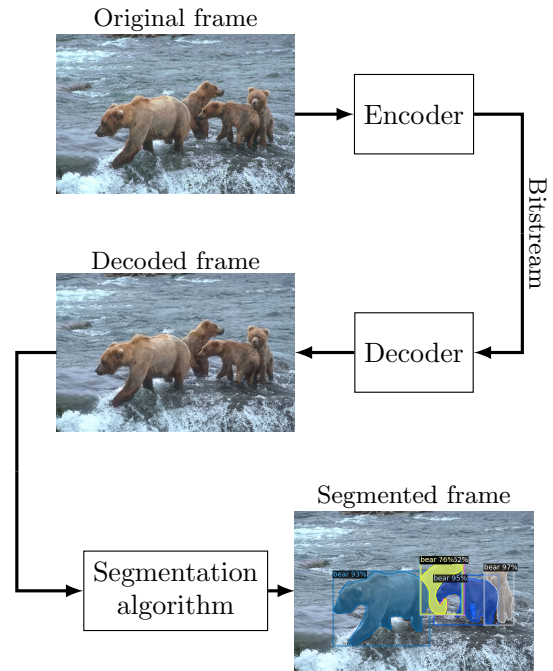


Fig. 1: Exemplary VCM scenario for image segmentation.

instead of a human. That question can be counted to the area of video coding for machines (VCM), for which MPEG founded an ad hoc group in 2019 targeting a possible standardized VCM bitstream format [4] [5]. Such a VCM scenario is shown in Figure 1 for the image segmentation task, which aims to cut out instances of objects, e.g. bears, as accurately as possible. There, the VCM task is to reduce the bitstream size while still being able to properly segment the objects in the decoded frame.

In a recent research [6], we have discovered that the coding gains of VVC over HEVC are smaller when measuring for a VCM scenario compared to a classic scenario using quality metrics representing the human visual system. Additional experiments showed that some in-loop filters such as the adaptive loop filter, which increase the visual quality for humans, harm the coding performance when considering the detection accuracy of a neural object detection network.

Following these results, we now propose a rate-distortion optimization (RDO) for VVC that is specially designed to achieve higher coding gains in VCM scenarios compared to standard VVC encoding. To that extent, we substitute the

commonly used sum of squared errors (SSE) metric with distortion metrics that are calculated in the feature space generated with the first few layers of a neural network. We call this method feature-based RDO (FRDO), which is then taken to derive the best block partitioning decisions when the decoded frame is analyzed by an algorithm. We focused on the block partitioning since this was stated to be responsible for around a third of VVC coding gain against HEVC in [7]. By only influencing the encoder decisions, we assure that the resulting bitstream is still standard-compliant.

There already exist other approaches to improve the coding performance for VCM scenarios. In [8], the authors published a saliency-driven extension to the x265 codec where they reduced the quality in image areas that a saliency detection network had classified as unlikely to contain an object. A similar approach has been presented in [9], where the authors used the early layers of an object detector to generate a saliency map which is used to assign fewer bits in HEVC to areas that are probably not important for object detection. A major drawback of such saliency-driven approaches is that the coding performance highly depends on the used saliency detection algorithm.

In contrast to this, our approach directly considers the influence of compression artifacts and information loss on a neural network and its convolution and pooling layers. This takes place inside the encoder and on a block-based level. Furthermore, the whole frame is encoded with the same quality and block partitioning is derived from feature space.

The remainder of this paper is structured as follows: in the subsequent chapter, the conventional RDO and the block partitioning in VVC are discussed. In Chapter III, the proposed FRDO is explained in detail. The results of the conducted experiments to compare the proposed FRDO against the conventional RDO in a VCM scenario are presented in Chapter IV before concluding the paper.

II. RATE DISTORTION OPTIMIZATION AND BLOCK PARTITIONING IN VVC

A. Rate Distortion Optimization as Lagrangian Optimization

For each block of an input sequence, the video encoder searches for the best possible coding parameter configuration ϕ that results in a block of distorted pixels \tilde{B}_ϕ . To that end, the distortion D has to be kept small by not exceeding a bitrate limit R_{\max} which can be expressed according to [10] as

$$\min_{\phi} D(\phi) \quad \text{s.t.} \quad R(\phi) \leq R_{\max}, \quad (1)$$

with $R(\phi)$ representing the rate that is required to transmit the coefficients of the transformed and quantized pixel error of \tilde{B}_ϕ and the metadata to signal ϕ to the decoder side.

This optimization problem can be solved by a Lagrangian relaxation that balances the distortion and the rate with the Lagrange multiplier λ by

$$J(\phi) = D(\phi) + \lambda \cdot R(\phi), \quad (2)$$

where the encoder tests different parameter configurations ϕ and chooses the configuration resulting in the lowest costs $J(\phi)$ for a given value of λ .

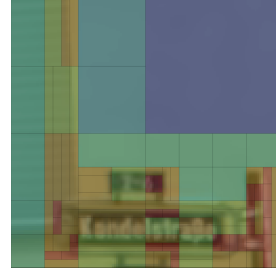


Fig. 2: Block structure for an exemplary CTU of size 128×128 pixels, which has been coded with VTM and a QP of 22. A warmer color represents a higher depth in the recursion tree.

Depending on the choice of λ , the RDO can be regulated towards a higher quality or a lower rate. When increasing λ , the encoder prefers a parameter configuration ϕ which results in a lower rate. When decreasing λ , the encoder will find a ϕ which delivers a lower distortion. The Lagrange multiplier λ is calculated from the user-defined quantization parameter (QP) according to [11] and [12] by

$$\lambda = k \cdot 2^{(QP-12)/3}, \quad (3)$$

where k is a constant, which is determined experimentally for each codec standard and each frame type. In the VVC test model (VTM) implementation 8.0 [3], k is typically set to 0.57 for I-slices.

In most hybrid video coding standards, the distortion term D for the RDO is measured with the SSE between the reconstructed pixels of a block \tilde{B}_ϕ and the corresponding original pixels B_{orig} by

$$D_{\text{SSE}}(\phi) = \sum_{(x,y) \in B} (B_{\text{orig}}[x,y] - \tilde{B}_\phi[x,y])^2, \quad (4)$$

where x and y denote pixel indices for \tilde{B}_ϕ and B_{orig} .

Additionally, the rate R has to be calculated for each reconstructed block in order to calculate its costs J . Eventually, the parameter configuration ϕ resulting in the lowest costs is chosen by the encoder.

Multiple approaches already exist aiming to optimize the RDO for different use case scenarios. In [13], the authors stated that the visual impression of the human is different from the image fidelity which is measured by the SSE. Therefore, they used a hybrid approach combining the SSE distortion measurement with the structural similarity index (SSIM) to increase the subjective quality while still preserving the image fidelity. Another approach considers the maximum pixel error instead of the SSE which showed superior results for medical content [14]. Lastly, the authors in [15] proved that it is possible to decrease the decoding energy when adding an estimated decoding energy term to the RDO.

B. Block Partitioning in VVC with RDO

In VVC, each frame is separated into coding tree units (CTUs) with a size of 128×128 pixels [3]. These CTUs are used as the root of a quad-tree, which equally separates the CTUs recursively into four squared coding units (CUs). Thereupon, each leaf of the quad-tree can be further divided into non-squared CUs by a nested multi-type tree, which is

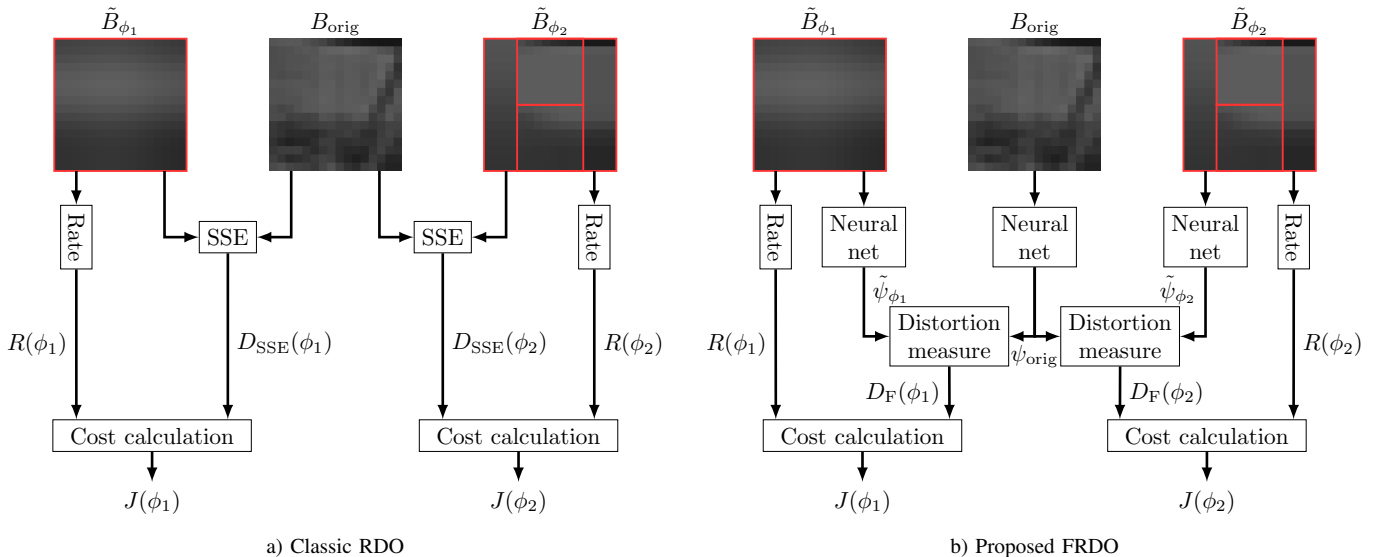


Fig. 3: Comparison between RDO with FRDO for two reconstructed blocks \tilde{B} from original block B_{orig} , resulting from two different parameter configurations ϕ_1 and ϕ_2 . The red lines indicate the block partitioning.

new compared to HEVC. The multi-type tree allows binary and ternary splits in horizontal and vertical direction so that the encoder is able to adapt the CUs more precisely to the frame content. This recursive procedure can split the CUs up to a size of 4×4 pixels. An exemplary VVC block partitioning for a CTU is depicted in Figure 2, where it can be seen that homogeneous areas are covered with large CU sizes, whereas the encoder chooses smaller CUs in areas with more detailed content such as the street sign in the bottom part. The binary and ternary splits result in non-squared CUs, which allow the encoder more freedom to adapt the block partitioning to the content.

In order to achieve the best possible CTU partitioning in terms of RDO, each CU of the size $M \times N$ is compared against a CU of the same size, which has been split differently into sub-CUs as it can be seen for the corresponding coding blocks \tilde{B}_ϕ in Figure 3a. For both CUs the best parameter configuration, which contains the prediction and the transform mode, has already been determined before, and thus the distortion and the rate including the additional bits for signaling the splits can be calculated. Then, the CU with the lower costs will be used for further processing in the coding tree at larger CU sizes. This procedure starts at the deepest recursion level leaves with small CU sizes, and moves up to the quad-tree root until the complete CTU is partitioned.

III. PROPOSED FEATURE-BASED RDO

A. Introduction to FRDO

Most neural networks take the input information from pixel space and transform this information into a denser and more abstract feature space by convolution and pooling layers. From this compact feature space, the neural network derives decisions with the help of attached fully-connected and softmax layers, e.g. to locate or classify objects. Therefore, the task of VCM is to preserve a high feature fidelity rather than a high pixel fidelity. However, while a high pixel fidelity automatically leads to a high feature-fidelity, the reverse is

not the case, since a high feature fidelity does not necessarily require a high pixel fidelity. The proposed FRDO aims at exploiting this gap in order to reduce the required rate.

As shown in Figure 3b, the first step of FRDO transforms each coding block B_ϕ and the corresponding original block B_{orig} into the feature space. For that purpose, the first convolution, Rectified Linear Unit (ReLU), and pooling layers of an arbitrary trained classification or detection network are fed with the block content, which can be formulated as

$$\psi_\phi = f(B_\phi), \quad (5)$$

with $f(\cdot)$ and ψ_ϕ representing the used neural network and the resulting three-dimensional feature map, respectively. The reasons for only using the first layers of a neural network to derive the feature space are twofold. First, the runtime is reduced. Second, the spatial resolution is decreased by the subsequent convolution and pooling layers, which makes deep networks unfeasible to apply to small coding blocks. Even by zero-padding small input patches, e.g. 4×4 pixels in VVC, these padded patches then consist of a significant number of zeros which is likely to falsify the distortion measurement.

B. Calculating Distortions in Feature Space

Now, the feature map $\tilde{\psi}_\phi$ derived from the reconstructed block \tilde{B}_ϕ can be compared against the feature map ψ_{orig} derived from the original block B_{orig} . With that, a distortion can be measured in this feature space similar to (4) by

$$D_{\text{FSSE}}(\phi) = \sum_{(x,y,c) \in \psi} (\psi_{\text{orig}}(x,y,c) - \tilde{\psi}_\phi(x,y,c))^2, \quad (6)$$

with x , y , and the channel index c representing the pixel-wise access to each element of ψ_{orig} and ψ_ϕ in the feature space.

Finally, this new feature-based distortion measure D_{FSSE} allows to reformulate the RDO cost calculation from (2) as FRDO for each parameter configuration ϕ as

$$\min_{\phi} J(\phi) = D_{\text{FSSE}}(\phi) + \lambda \cdot R(\phi). \quad (7)$$

As generally known, SSE tends to focus on large errors by neglecting smaller ones because of the square operation. Thus, we also propose a feature-based sum of absolute differences (FSAD), which can be formulated as

$$D_{\text{FSAD}}(\phi) = \sum_{(x,y,c) \in \psi} |\psi_{\text{orig}}(x,y,c) - \tilde{\psi}_{\phi}(x,y,c)|. \quad (8)$$

A comparison between the feature-based distortion metrics is provided in Section IV.

C. Adapt Feature-Based Distortion Measure to λ

As shown in (2) and (7), RDO and FRDO both depend on a carefully chosen Lagrange multiplier λ . The λ used in the VTM encoder is optimized for SSE. However, the proposed feature-based distortion D_{F} can be located in a different range of values than D_{SSE} , which might lead to sub-optimal coding decisions. To relieve this problem, we scale the feature-based distortion derived from the first parameter configuration ϕ_1 to the equivalent SSE by

$$D_{\text{F}}^*(\phi_1) = D_{\text{F}}(\phi_1) \cdot \frac{D_{\text{SSE}}(\phi_1)}{D_{\text{F}}(\phi_1)} = D_{\text{SSE}}(\phi_1), \quad (9)$$

which results in the feature-based distortion and the SSE for a block coded with ϕ_1 having the same value. The feature-based distortion of the second coding block is multiplied with the same factor, in order to preserve the relative differences by

$$D_{\text{F}}^*(\phi_2) = D_{\text{F}}(\phi_2) \cdot \frac{D_{\text{SSE}}(\phi_1)}{D_{\text{F}}(\phi_1)}. \quad (10)$$

With this mapping, the feature-based distortion is adapted to λ by still being able to compare the two coding blocks according to their influence on a neural network, without having to re-evaluate λ for the proposed distortion measures.

With this normalized distortion and since it was shown in [13] and [15] that it is beneficial to not completely omit the common SSE as distortion, we also propose a hybrid FRDO (HFRDO) version that equally combines D_{SSE} and a normalized feature-based distortion D_{F}^* by

$$J(\phi) = 0.5 \cdot (D_{\text{SSE}}(\phi) + D_{\text{F}}^*(\phi)) + \lambda \cdot R(\phi). \quad (11)$$

D. Applying FRDO in Hybrid Video Codec

FRDO can substitute every RDO in common hybrid video codecs where coding parameter configurations ϕ and thus the corresponding coding blocks are compared to each other. In this paper, we focus on the block partitioning as explained in Section II-B to save complexity.

In further experiments, we also allow the encoder to vary the QP for each CU in a certain range, by using the FRDO. There, the encoder partitions a CTU into the blocks for different QP values, and chooses the best QP in terms of rate and distortion afterwards. With that, the coding decisions can be even better adapted to neural networks at the drawback of increased encoding complexity depending on the allowed QP range.

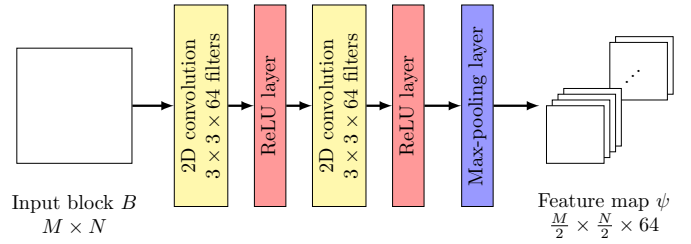


Fig. 4: Extracting the feature map ψ from a block of pixels B with the first five VGG-16 layers.

IV. EXPERIMENTAL RESULTS

A. Simulation Setup

In order to evaluate the proposed FRDO, we added it to VTM 8.0 [3] and compared this FRDO VTM against the unmodified version with conventional RDO. We only applied the FRDO to the luminance channel. To derive the feature space for FRDO, we used a pre-trained VGG-16 [16] model from the Pytorch vision package in version 0.5.0 [17] that is actually used to classify images. From this model, we used the first five layers as shown in Figure 4. In order to measure the coding performance for neural networks, we compressed the 500 validation images of the Cityscapes [18] dataset, which contains street views with annotated road users, with QP values in all intra configuration. Subsequently, each compressed frame is fed into Mask R-CNN [19] to detect and extract all road users. The extracted objects are compared against the ground-truth instances with the mean average precision (mAP) metric as described in [18] and implemented in [20] that directly measures the segmentation performance of Mask R-CNN. Similar to [6], we weight the average precision (AP) according to the number of instances of each classes in the validation set, since some classes such as bus and truck are underrepresented in Cityscapes compared to the classes car and person. Because of that, weighting all classes equally would lead to a deformed result. For Mask R-CNN, we chose the model with a ResNet50 backbone from the Detectron2 model zoo [21], which has already been trained on the Cityscapes dataset. By using a validation network that differs in structure and weights from the VGG-16 network to obtain the feature space, we want to show the universal applicability of FRDO without any knowledge of the finally used network in the application case.

B. Comparison FRDO with RDO

In Figure 5, the weighted AP for Mask R-CNN is plotted over the required bitrate for conventional RDO as reference and FRDO with the different distortion metrics. We selected a QP range from 12 to 27 in steps of 5, because for most practical applications the accuracy loss caused by compression should not be too high compared to the case with uncompressed input data (dotted line).

It can be seen from the red curve that FRDO with SSE as distortion measure in the feature space is not able to significantly reduce the required bitrate compared to the blue curve representing the standard VTM with normal RDO. The green curve representing the proposed FRDO with SAD

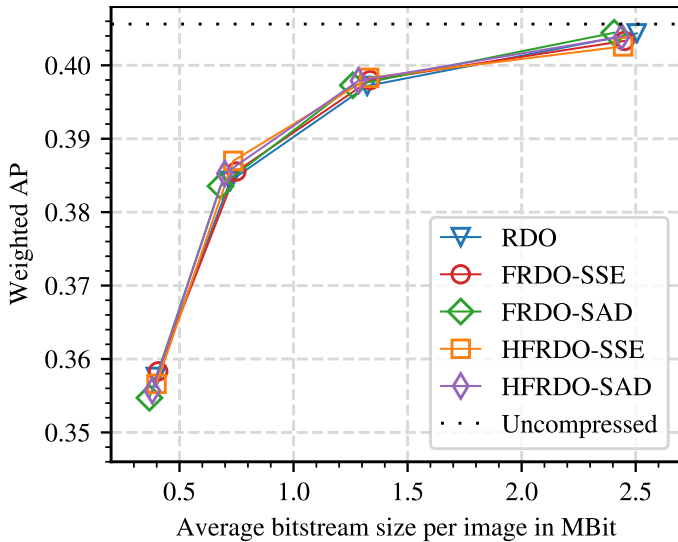


Fig. 5: Weighted AP values over bitrates comparing the different RDOs. Values are averaged over the 500 Cityscapes validation images for $QP \in \{12, 17, 22, 27\}$.

TABLE I: BDR with respect to the particular quality metric using VTM with conventional RDO as anchor for $QP \in \{12, 17, 22, 27\}$.

Optimization method	Quality metric	
	PSNR	Weighted AP
FRDO-SSE	4.30 %	-0.50 %
FRDO-SAD	3.02 %	-3.99 %
HFRDO-SSE	1.63 %	-4.55 %
HFRDO-SAD	1.26 %	-5.49 %

requires less bitrate than RDO, while maintaining a similar detection rate for high bitrates. With decreasing bitrate, the FRDO with SAD is not able to keep the same detection rate as the reference. The resulting bitrate for the measurement points of the hybrid FRDO as introduced in (11) with SAD are located, as expected, between the points for RDO and FRDO-SAD.

In order to quantify the coding performance of the different FRDO versions, the Bjøntegaard delta rate (BDR) [22] values are listed in Table I for the curves shown in Figure 5. The BDR values with respect to the PSNR represent the bitrate savings at a fixed quality for the human visual system. Calculating the BDR with respect to the weighted AP returns the bitrate savings at a fixed detection rate for Mask R-CNN. Thereby, a negative number expresses savings compared to the anchor.

From this table, it can be seen that the FRDO with SSE reduces the required bitrate by 0.5 % for the same detection accuracy. Using FRDO-SAD decreases the bitrate by 3.99 %. These results indicate that SAD is better suited to represent distortions in the feature space than SSE. At the same time, the coding performance measured with PSNR decreases for the FRDO variants, which proves that the proposed FRDO can preserve the feature space even though it significantly reduces the pixel-fidelity. Using the hybrid FRDO with SSE achieves coding gains of 4.55 % compared to the standard RDO in VTM. Using the HFRDO-SAD results in the best coding performance for the VCM task with 5.49 % bitrate savings. Compared to FRDO, the hybrid variants show higher

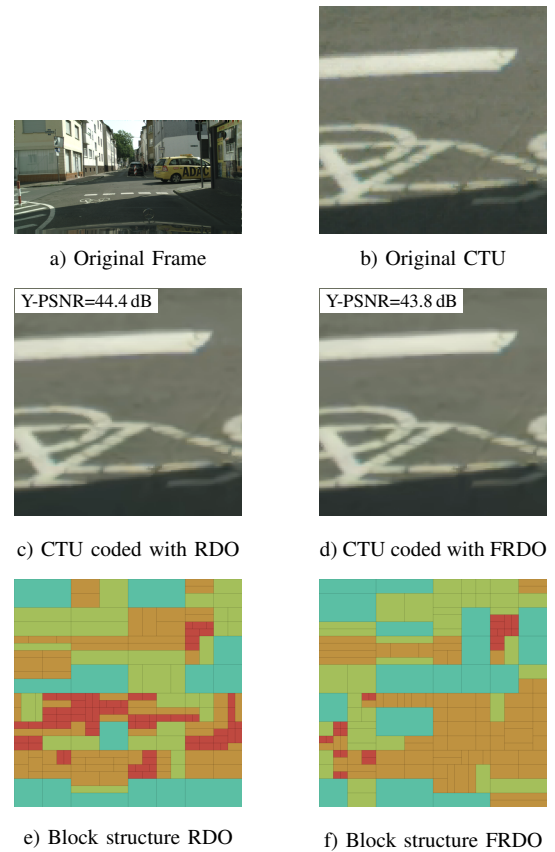


Fig. 6: Comparison of one exemplary CTU out of Cityscapes image *frankfurt_000000_000294_leftImg8bit.png* compressed with RDO (left) and FRDO with SAD (right) and a static QP of 22. A warmer color represents a higher depth in the recursion tree.

coding gains for mAP and do not harm the classic coding performance for PSNR that much.

In Figure 6, the block partitioning with RDO and FRDO with SAD is compared for a CTU that does not contain a relevant object. With FRDO, the block structure is not as deep as for the same CTU coded with RDO, which results in bitrate savings. Yet, the pixel-fidelity and also the visual quality is slightly better for the CTU compressed with RDO.

C. FRDO with Delta QP

In another experiment, we also allowed the encoder to vary the base QP in a range of -3 to $+3$ for each CU according to the used RDO and plotted the rate-weighted-AP diagram in Figure 7. The corresponding BDR values compared to the anchor RDO without delta QP are listed in Table II. By using the proposed FRDO with SAD, 5.35 % of bitrate can be saved for the same detection accuracy of the Mask R-CNN compared to the standard VTM. Contrary, to obtain the same PSNR as the anchor, the bitrate has to be increased by 4.55 %, which again indicates that the proposed FRDO preserves, as desired, the detection rate rather than the pixel-fidelity. When allowing delta QP , the hybrid FRDO with SAD even further increases the coding gains for the VCM scenario up to 9.95 %. In contrast, allowing delta QP for conventional RDO only results in 1.15 % rate savings for the VCM scenario, which

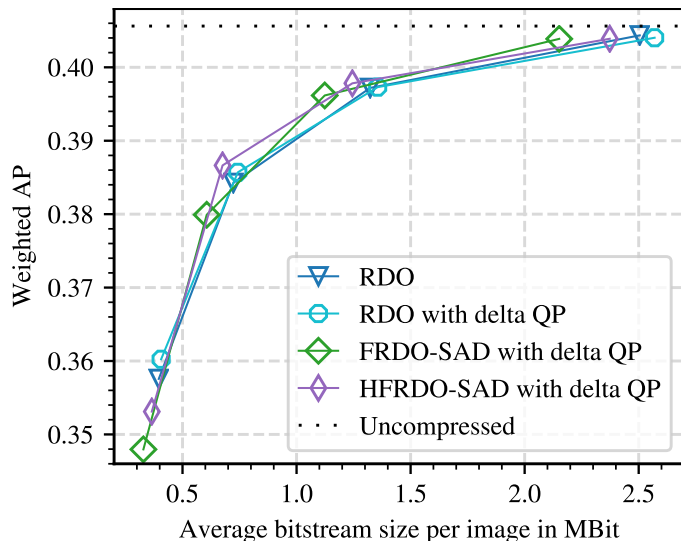


Fig. 7: Weighted AP values over bitrates comparing the different RDOs when allowing delta QP . Values are averaged over the 500 Cityscapes validation images for $QP \in \{12, 17, 22, 27\}$.

TABLE II: BDR with respect to the particular quality metric when allowing a delta QP between -3 and 3 using VTM with conventional RDO without delta QP as anchor for $QP \in \{12, 17, 22, 27\}$.

Optimization method	Quality metric	
	PSNR	Weighted AP
RDO with delta QP	-0.36 %	-1.15 %
FRDO-SAD with delta QP	4.55 %	-5.35 %
HFRDO-SAD with delta QP	1.01 %	-9.95 %

proves that the coding gains are mainly achieved by the FRDO and not only by allowing delta QP .

V. CONCLUSION

In this paper, a novel feature-based RDO for VCM scenarios has been presented that returns a standard-compliant bitstream optimized for neural networks. With this FRDO, the encoder aims to achieve a high feature-fidelity rather than a high pixel-fidelity. This results in bitrate savings when the detection accuracy of a neural segmentation network is taken to evaluate the coding quality instead of metrics trying to represent the human visual system. In a VCM scenario with the Mask R-CNN network as final detector, HFRDO is able to save up to 5.49 % bitrate compared to the standard RDO in VTM-8.0. A drawback in this case is the increased encoder runtime of around 2.3, when encoding with FRDO compared to standard VTM. Allowing the encoder with HFRDO-SAD to vary the QP for each CU, further reduces the required bitrate up to 9.95 %. Using the VGG-16 network to obtain the feature space that differs from the final evaluation network in structure and weights, indicates the universal applicability of FRDO. Nevertheless, it would be interesting in future work to create the feature space for FRDO with the first few layers of the evaluation network. This can serve as oracle test to see whether the coding performance can be even further increased, when the encoder is adapted to the evaluation network. Besides, FRDO could also be applied in other encoder parts and it could also be tested for inter-coding with a suitable dataset.

REFERENCES

- [1] G. J. Sullivan, J.-R. Ohm, W.-J. Han, and T. Wiegand, "Overview of the high efficiency video coding (HEVC) standard," *IEEE Transactions on Circuits and Systems for Video Technology*, vol. 22, no. 12, pp. 1649–1668, Sep. 2012.
- [2] B. Bross, J. Chen, S. Liu, and Y. Wang, "JVET-Q2001: Versatile video coding (draft 8)," Joint Video Exploration Team (JVET) of ITU-T SG 16 WP 3 and ISO/IEC JTC 1/SC 29/WG 11, Brussels, Belgium, Tech. Rep., Jan. 2020.
- [3] J. Chen, Y. Ye, and S. Kim, "JVET-Q2002: Algorithm description for versatile video coding and test model 8 (VTM 8)," Joint Video Exploration Team (JVET) of ITU-T SG 16 WP 3 and ISO/IEC JTC 1/SC 29/WG 11, Brussels, Belgium, Tech. Rep., Jan. 2020.
- [4] Y. Zhang and P. Dong, "MPEG-M49944: Report of the AhG on VCM," Moving Picture Experts Group (MPEG) of ISO/IEC JTC1/SC29/WG11, Geneva, Switzerland, Tech. Rep., Oct. 2019.
- [5] L. Duan, J. Liu, W. Yang, T. Huang, and W. Gao, "Video coding for machines: A paradigm of collaborative compression and intelligent analytics," *ArXiv*, vol. abs/2001.03569, 2020.
- [6] K. Fischer, C. Herglotz, and A. Kaup, "On intra video coding and in-loop filtering for neural object detection networks," in *Proc. IEEE International Conference on Image Processing (ICIP)*, Oct. 2020, pp. 1147–1151.
- [7] A. Wieckowski, J. Ma, V. George, H. Schwarz, D. Marpe, and T. Wiegand, "Generalized binary splits: A versatile partitioning scheme for block-based hybrid video coding," in *Proc. Picture Coding Symposium (PCS)*, Nov. 2019, pp. 1–5.
- [8] L. Galteri, M. Bertini, L. Seidenari, and A. Del Bimbo, "Video compression for object detection algorithms," in *Proc. International Conference on Pattern Recognition (ICPR)*, Aug. 2018, pp. 3007–3012.
- [9] H. Choi and I. V. Bajic, "High efficiency compression for object detection," in *Proc. IEEE International Conference on Acoustics, Speech and Signal Processing (ICASSP)*, Apr. 2018, pp. 1792–1796.
- [10] G. Sullivan and T. Wiegand, "Rate-distortion optimization for video compression," *IEEE Signal Processing Magazine*, vol. 15, no. 6, pp. 74–90, Nov. 1998.
- [11] T. Wiegand, G. Sullivan, G. Bjontegaard, and A. Luthra, "Overview of the h.264/AVC video coding standard," *IEEE Transactions on Circuits and Systems for Video Technology*, vol. 13, no. 7, pp. 560–576, Jul. 2003.
- [12] B. Li, J. Xu, D. Zhang, and H. Li, "QP refinement according to Lagrange multiplier for high efficiency video coding," in *Proc. IEEE International Symposium on Circuits and Systems (ISCAS)*, May 2013, pp. 477–480.
- [13] Q. Wang, H. Yuan, J. Huo, and P. Li, "A fidelity-assured rate distortion optimization method for perceptual-based video coding," in *2019 IEEE International Conference on Image Processing (ICIP)*, Aug. 2019, pp. 4135–4139.
- [14] K. Jaskolka and A. Kaup, "Improving the rate-distortion model of HEVC intra by integrating the maximum absolute error," in *Proc. IEEE International Conference on Acoustics, Speech and Signal Processing (ICASSP)*, May 2019, pp. 1817–1821.
- [15] C. Herglotz, A. Heindel, and A. Kaup, "Decoding-energy-rate-distortion optimization for video coding," *IEEE Transactions on Circuits and Systems for Video Technology*, vol. 29, no. 1, pp. 171–182, Jan. 2019.
- [16] K. Simonyan and A. Zisserman, "Very deep convolutional networks for large-scale image recognition," in *Proc. International Conference on Learning Representations (ICLR)*, May 2015.
- [17] Pytorch, "torchvision," <https://github.com/pytorch/vision>, 2020.
- [18] M. Cordts, M. Omran, S. Ramos, T. Rehfeld, M. Enzweiler, R. Benenson, U. Franke, S. Roth, and B. Schiele, "The cityscapes dataset for semantic urban scene understanding," in *IEEE Conference on Computer Vision and Pattern Recognition (CVPR)*, Jun. 2016, pp. 3213–3223.
- [19] K. He, G. Gkioxari, P. Dollár, and R. B. Girshick, "Mask R-CNN," in *Proc. IEEE International Conference on Computer Vision (ICCV)*, Oct. 2017, pp. 2980–2988.
- [20] M. Cordts and M. Omran, "The cityscapes dataset," <https://github.com/mcordts/cityscapesScripts>, 2017.
- [21] Y. Wu, A. Kirillov, F. Massa, W.-Y. Lo, and R. Girshick, "Detectron2," <https://github.com/facebookresearch/detectron2>, 2019.
- [22] G. Bjontegaard, "Calculation of average PSNR differences between RD-curves," *ITU-T Video Coding Experts Group (VCEG)*, Apr. 2001.